How to Cite: Ibrayev, N.Kh., & Seliverstova, E.V. (2023). Interaction of the Excited Electronic States of Carbon Quantum Dots and Molecular Oxygen. *Eurasian Journal of Chemistry, 111(3), 60-68.* https://doi.org/10.31489/2959-0663/3-23-17

Article

Received: 31 May 2023 | Revised: 30 June 2023 |
Accepted: 18 July 2023 | Published online: 31 July 2023

UDC 535.37+544.4

https://doi.org/10.31489/2959-0663/3-23-17

Niyazbek Kh. Ibrayev*, Evgeniya V. Seliverstova

Institute of Molecular Nanophotonics, Karaganda University of the name of academician E.A. Buketov, Karaganda, Kazakhstan
*(*Corresponding author's e-mail: niazibrayev@mail.ru)*

Interaction of the Excited Electronic States of Carbon Quantum Dots and Molecular Oxygen

The S,N-doped carbon quantum dots based on citric acid and L-cysteine were synthesized. The sizes of the synthesized carbon dots vary from 4 to 10 nm. The absorption spectrum exhibits a band with a maximum at 360 nm, as well as a shoulder at about 240–250 nm. The fluorescence band of the studied carbon dots is located in the region of 370–600 nm with a maximum at ~430 nm. The properties of the long-lived luminescence of carbon quantum dots solutions were studied. It was established that the decay of triplet states occurs as a result of a radiative phosphorescent transition and triplet–triplet annihilation. The synthesized carbon quantum dots are reviled to be the singlet oxygen sensitizers, as evidenced by the observed luminescence of molecular oxygen upon excitation of solutions in the absorption band of the carbon quantum dots. It was shown that when O_2 ($^3\Sigma_g^-$) was added to the solution, the process of singlet–triplet annihilation develops, the efficiency of which depends on the concentrations ratio of triplet carbon quantum dots and singlet $O_2(^1\Delta_g)$ molecules. In the presence of plasmonic Ag nanoparticles, the phosphorescence of singlet oxygen is enhanced.

Keywords: carbon quantum dots, singlet oxygen, excited states, delayed fluorescence, phosphorescence, Ag nanoparticles, plasmons.

Introduction

Molecular oxygen (O_2) is an oxidizing agent that is involved in metabolic pathways that are fundamental to aerobic life. However, the oxidizing power of O_2 at room temperature is low due to the strong oxygen-oxygen chemical bond, as well as its triplet nature of the ground state. These difficulties can be overcome by transferring oxygen to the singlet state $O_2(^1\Delta_g)$ [1]. Oxygen activation is a very interesting task for biology, chemistry and industry. A great contribution to the development of electronic mechanisms for the activation of molecular oxygen was made by Minaev B.F. *et al.* [2–5].

To overcome the spin forbidding rule for the transition of O_2 to $O_2(^1\Delta_g)$, photosensitizers with a high yield to the triplet state are required. Photosensitization-generated reactive oxygen species $O_2(^1\Delta_g)$ can be used for various photodynamic applications, such as photodynamic therapy (PDT) [6–8], light deactivation of proteins [9], oxidative processes in biological objects [10, 11] and photodegradation of organic pollution [12].

Therefore, the photophysical properties of photosensitizers (spin-catalysts) have a great importance for the photosensitized activation of oxygen, especially the population of triplet states by intersystem crossing.

Carbon quantum dots (CQDs) are a promising type of photosensitizer. The CQDs refers to quasi-spherical or spherical particles with a diameter of less than 10 nm. They could be represented as a core/shell structure consisting of a carbon core with graphite fragments and a shell of various surface functional groups [13]. CQDs have attracted attention due to their unique properties and some advantages over organic molecules and traditional semiconductor quantum dots [14]. CQDs particles have chemical resistance and photo-stability, high luminescence efficiency, good biocompatibility, and low toxicity. This causes their wide application in such areas as bioimaging [15], protective coatings [16], LEDs, solar cells [17], lasers [18] and sensors [19].

CQDs along with fluorescence exhibit an additional afterglow that is also an undoubted advantage. Moreover, the efficiency and position of the bands of both types of CQDs luminescence on the wavelength scale can be controlled by the directed synthesis [13, 16]. In this regard, CQDs particles are an attractive agent for PDT in deep tissues with controlled optical properties through chemical functionalization [16–19]. CQDs were shown as effective PDT agents in antibiotic therapy and wound healing, despite of low optical absorption and emission in the IR and near IR ranges [20, 21].

In view of extensive research of the CQDs exhibiting photodynamic effects inducing cytotoxicity in cancer cells and tumors, the fundamental understanding of parameters that allow CQDs to be useful PDT agents remains unclear. In [22], the role of oxygen-containing chemical groups in the catalytic generation of OH radicals, one of the common types of reactive oxygen species, was illustrated. However, the detailed mechanism of the photodynamic activity of CQDs has rarely been reported [23, 24].

The plasmonic effect is currently actively used to increase the efficiency of photo-processes both in organic molecules [25–28] and in semiconductor quantum dots [29], since the rates of photo-physical reactions could be changed near the plasmonic nanoparticles (NPs) surface [25, 30–31].

For CQDs, the plasmonic effect was used to enhance fast fluorescence [32–36]. The authors of [36] demonstrated that, by chemically binding CQDs to gold NPs, it is possible to achieve a fivefold enhancement of the orange emission of carbon dots. The observed intensity grow is due to the ultrafast resonant energy transfer from the gold NP to the carbon dot. Composites based on CQDs and plasmonic metal NPs were used to detect mercury ions [37], chlorophyll [38], bioimaging [39], anticancer drug [40], etc.

This paper presents the results of our study of the singlet oxygen photosensitization by CQDs, as well as the plasmon effect of NPs on these processes. The both electronic mechanisms of intermolecular interactions between the triplet CQDs and also — CQDs species with molecular oxygen are considered.

Experimental

For the CQDs synthesis the citric acid (CA, Sigma Aldrich) was used as a carbon source, and L-cysteine (Sigma Aldrich) was chosen as a source of N- and S-containing groups. All reagents were of analytical grade and used without further purification. The microwave reactor Monowave 200 (Anton Paar) was used for the preparation of CQDs. To do this, CA and L-cysteine were diluted with deionized water (5 mL) in a borosilicate glass tube and sonicated for 30 minutes. Next, the tube was placed in a microwave reactor and heated at 200 °C for an hour with vigorous stirring. The molar ratio of citric acid:L-cysteine was 1:2. After that solutions with different concentrations of ethanol were prepared. Its volume fraction was 25, 50, or 75 %. In the CQDs+Ag NPs solutions the concentration of CQDs was constant, and the concentration of plasmonic NPs was 10^{-14}, 10^{-13} or 10^{-12} mol/L.

Silver NPs were obtained in solution by ablation of a silver target by high-intensity laser radiation from a Nd:YAG laser with a generation wavelength (λ_{gen}) of 532 nm, a pulse duration τ_{pulse}=8 ns, and a pulse energy E~90 mJ. The laser beam was focused by a converging lens onto a target immersed in ethanol. The diameter of the laser spot on the target was 0.01 cm^2. The height of the solvent above the target was 0.8 cm. The diameter of the resulting NPs was 46±12 nm (Zetasizer S90, Malvern). SEM images (Mira 3LMU, Tescan) showed that the NPs have a spherical shape (Fig. 1).

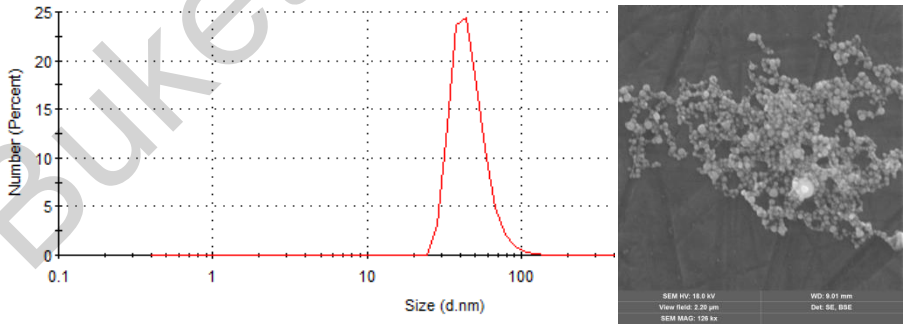

Figure 1. Size distribution and SEM image of Ag NPs

Absorption spectra were obtained using a Cary 300 spectrophotometer (Agilent Techn.). Fast and long-lived luminescence spectra were recorded using a Cary Eclipse spectrometer (Agilent Techn.).

Fluorescence decay kinetics was measured on a spectrofluorometer with picosecond resolution and registration in the time-correlated single photon counting mode from Becker&Hickl. The excitation of the samples was carried out using a diode laser with λ_{gen}=375 nm, τ_{pulse}=120 ps. Fluorescence lifetimes were estimated with SPCImage software (Becker&Hickl).

Long-lived luminescence was recorded with an FLS1000 luminescence spectrometer (Edinburgh Instr.) equipped with highly sensitive UV-Vis (R13456, Hamamatsu) and IR (H10330C-75, Hamamatsu) photodetectors. Photoexcitation of samples at λ_{exc}=360.8 nm was carried out using a laser system based on Nd:YAG

laser LQ529, parametric light generator LP604 and second harmonic generator LG305. For the long-lived luminescence registration the cuvette with the CQDs solution was evacuated to a pressure of P = 10^{-5} mm Hg.

Results and Discussion

The absorption spectra of the studied CQDs are shown in Figure 2. The spectrum exhibits a weak band with a maximum at 360 nm, as well as a strong shoulder at about 240–250 nm. The long-wavelength absorption band is associated with π→π* transitions in aromatic compounds of the CQD, while the absorption at 200 nm and the shoulder at 250 nm are associated with n→σ* and n→π* transitions, respectively. As shown in [41], the intensity and position of the maximum of the CQD fluorescence band depend on the excitation wavelength (λ_{exc}). The most intense emission was registered for λ_{exc}=350 nm. Under these conditions, the fluorescence band is located in the region of 370–600 nm with a maximum at ~430 nm.

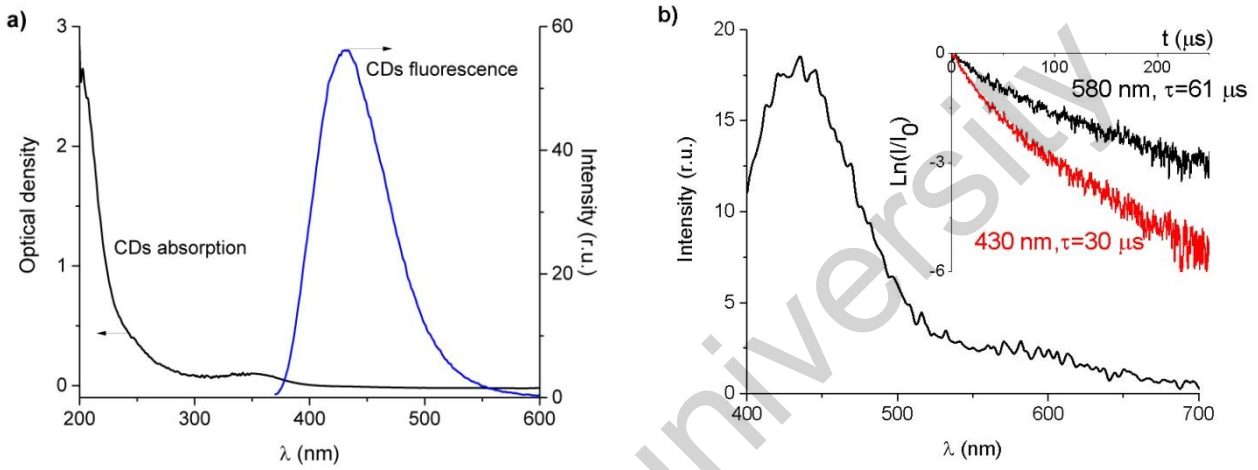

Figure 2. (*a*) Absorption (black curve) and fluorescence (blue curve, λ_{exc}=350 nm) spectra of CQDs and (*b*) long-lived luminescence of CQD in a solution with 25 % of ethanol.
The inset shows decay kinetics of long-lived luminescence detected at 430 nm and 580 nm. E_{exc}= 5.5 mJ

A broad band with two maxima at 430 and 580 nm was recorded in the long-lived luminescence spectrum (Fig. 2b). Since the short-wavelength band coincides in position and shape with the fast fluorescence spectrum, it can be concluded that it belongs to the delayed fluorescence (DF) of CQDs. The long wavelength band can be interpreted as phosphorescence. This is confirmed by the times estimated from the decay kinetics of the long-lived luminescence recorded at 430 and 580 nm. The duration of phosphorescence is almost 2 times longer than that for DF. Therefore, the DF can be of the triplet-triplet (T-T) annihilation nature. According to [42, 43], the presence of oxygen groups induces a decrease in ΔE_{ST} and an increase in the spin-orbit interaction in the CQD, which contributes to the population of triplet states.

It is known that the annihilation-type DF is a magnetically sensitive process [44], and its intensity depends quadratically on the intensity of the exciting light. To study the influence of the magnetic field on the DF of the CQDs species, we used the N35 neodymium magnet with a magnetic induction of ~1 T. The magnitude of the magnetic effect $g(B)$ was estimated from the relative change in the luminescence intensity in the presence and in the absence of a magnetic field using the following formula:

$$g(B) = \frac{I(B) - I(0)}{I(B)} \times 100\,\%, \qquad (1)$$

where I_B and I_0 are the luminescence intensities in the field and without the field, respectively.

As shown by the results (Table 1), in the presence of a magnetic field, the DF intensity decreases by ~33 %. The magnitude of the magnetic-field effect $g(B)$ decreases with increasing time of registration, which is apparently associated with a decrease in the number of triplet-excited particles. The intensity of the long-lived luminescence at λ_{reg}=580 nm is not significantly affected by the magnetic field.

Table 1

Values of magnetic effect *g(B)* on DF of the CQDs at various times of registration

№	Time of registration, μs	$g(B)$, % λ_{reg}= 430 nm
1	0	-33.2±3
2	5	-31.2±3
3	15	-28.6±3

The data presented in Figure 3 were obtained upon excitation of the CQDs solutions by laser pulses of various intensities. At a wavelength of 580 nm, the luminescence intensity linearly depends on the excitation energy, which is typical for phosphorescence. At λ_{reg}= 430 nm, the dependence $I_{DF} \sim I_{exc}^2$ indicates that the DF signal is a result of the T-T annhilation of the triplet carbon dots.

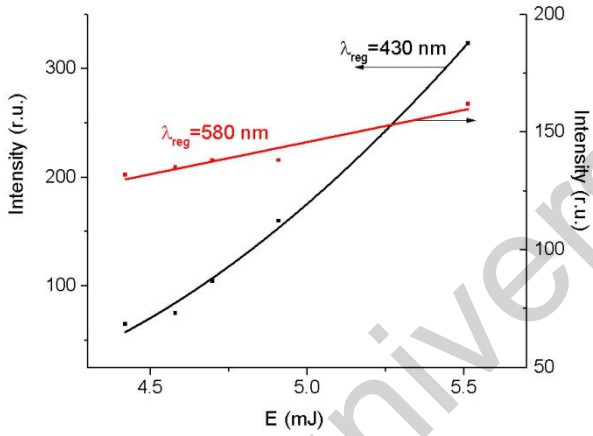

Figure 3. Dependence of the DF and phosphorescence intensity of CQDs on the energy (intensity) of the exciting light

Thus, the data obtained indicate that the photoexcitation of the CQDs solutions leads to formation of the excited CQDs triplet states (T_{CD}), as a result of singlet-triplet interconversion. These T_{CD} decay occurs as a result of the following processes:

$$T_{CD} \rightarrow S_0 + Phos., \quad (2)$$

$$T_{CD} + T_{CD} \rightarrow (T_{CD} \ldots T_{CD}) \rightarrow S_1 + S_0 \rightarrow 2S_0 + ADF, \quad (3)$$

where S_0, S_1, T_{CD} are the singlet and triplet electronic states of CQDs.

Reaction (2) is phosphorescence and expression (3) represents the reactions of triplet-triplet annihilation generating the delayed fluorescence (ADF).

CQDs are good sensitizers of singlet oxygen [22–24]. The efficiency of sensitization will be determined not only by the concentration of triplet CQDs, but also by the solvent [2, 3, 45–48]. Figure 4*a* shows the decay kinetics of the phosphorescence of singlet oxygen $O_2(^1\Delta_g)$ in water–ethanol solutions with different ethanol contents, measured at atmospheric pressure. With an increase in the proportion of ethanol, the intensity and lifetime of $O_2(^1\Delta_g)$ phosphorescence increase, since the oxygen concentration and the $O_2(^1\Delta_g)$ lifetime in ethanol are higher than in water [3, 45–48].

The results of experiments on the oxygen concentration effect on photo-processes in a water–ethanol solutions of CQDs are presented in Figure 4*b*. Before the start of measurements, the cuvette with the solution was evacuated to a pressure of $P = 10^{-5}$ mm Hg. In this case, there was no signal of oxygen phosphorescence at a wavelength of 1270 nm. With an increase in the concentration of $O_2(^3\Sigma_g^-)$ in the cell, the intensity of phosphorescence of $O_2(^1\Delta_g)$ increases (red curve). The lifetime within the measurement error remains constant and equal to τ_Δ = 9.2 μs. The DF signal of CQDs (black curve) was grew up with the addition of oxygen and reaches a maximum at $C(O_2)$ = 0.05 mL and then quenches. The DF lifetime of CQDs decreases with increasing $O_2(^3\Sigma_g^-)$ concentration (blue curve). The CQD's phosphorescence was quenched when initial oxygen concentrations were added to the solution, and we could not follow its dynamics, since water strongly scattered the exciting light.

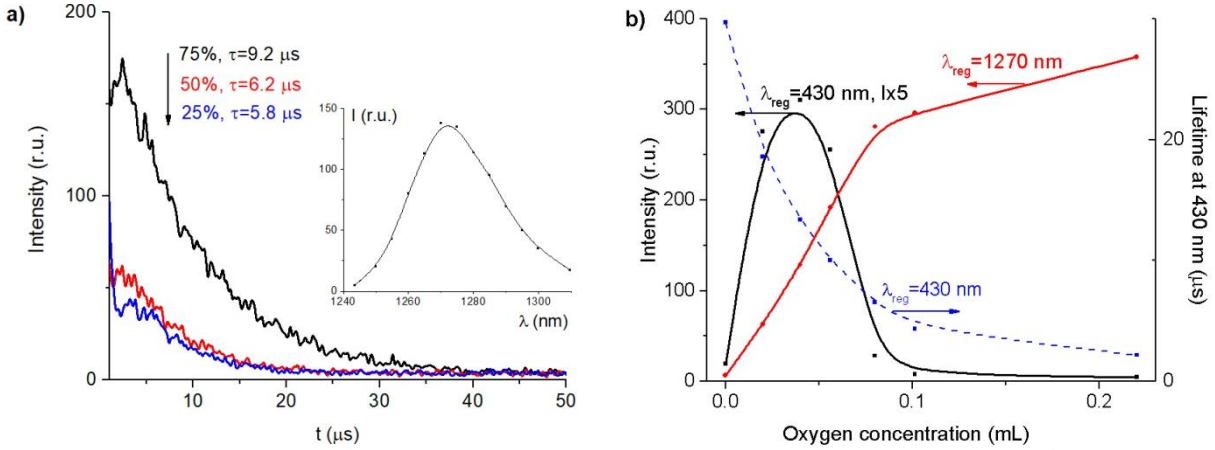

Figure 4. (*a*) Decay kinetics of $^1O_2$ phosphorescence (λ_{reg} = 1270 nm) sensitized by CQDs in solutions with different concentrations of ethanol at atmospheric pressure. The inset — the phosphorescence spectrum of $^1O_2$ (λ_{exc} = 350 nm) in a CQDs solution with 75 % ethanol. (*b*) Dependence of the intensity and lifetime of DF of CQDs (75 % ethanol) and $^1O_2$ phosphorescence (λ_{exc} = 350 nm) on the concentration of the oxygen

According to [1–3], the following processes can occur in collision complexes of molecular oxygen and CQD:

$$T_{CD} + (^3\Sigma_g^-) \rightarrow (T_{CD}\ ^3\Sigma_g^-)^{1,3,5} \rightarrow S_0 + {}^1\Delta_g \quad (4)$$

$$T_{CD} + {}^1\Delta_g \rightarrow (T_{CD}\ {}^1\Delta_g)^3 \rightarrow S_1 + {}^3\Sigma_g^- \rightarrow S_0 + {}^3\Sigma_g^- + h\upsilon_{DF} \quad (5)$$

$$^1\Delta_g \rightarrow {}^3\Sigma_g^- + h\upsilon_{Phos}, \quad (6)$$

where formula 4 — the reaction of singlet oxygen sensitization; formula 5 — the singlet–triplet annihilation reaction; formula 6 — the generation of singlet oxygen phosphorescence.

In accordance with reactions (4–6), the dependence of I_{DF} on the $O_2(^3\Sigma_g^-)$ concentration (Fig. 4*b*, black curve) is due to reaction 5. At low oxygen concentrations, the number of triplet CQDs is still sufficient to form pairs $(T_{CD}\ ^3\Sigma_g^-)^{1,3,5}$ which, decaying with the formation of S_1 states of CQDs, additionally generate DF. Under conditions of strong quenching of CQD triplets, the efficiency of the processes of both singlet–triplet (5) and intrinsic (3) annhilation decreases, which leads to a decrease in the CQD luminescence intensity.

In the presence of plasmonic NPs, the sensitization of singlet oxygen by organic dyes is enhanced [49, 50]. The next we consider the effect of Ag NPs on the activation of $O_2(^3\Sigma_g^-)$ molecules. The maximum absorption spectrum of silver NPs exhibits at 420 nm. At 250–270 nm, the absorption band of *d*-electrons of Ag appears. In the presence of plasmonic NPs, no change in the shape of the CQD absorption spectrum was observed. In this case, the optical density also practically did not change, both in the long-wavelength and short-wavelength absorption bands of the CQD.

At atmospheric pressure, the highest quenching of CQD's fluorescence was observed at $C_{Ag} = 10^{-12}$ mol/L. The decrease in intensity was about 11 % (Table 2). The fluorescence lifetime also decreases by 8–10 % on average. The observed decrease in the intensity and lifetime of CQD fluorescence in the presence of Ag NPs is associated both with the effect of plasmonic NPs on the radiative decay rate of CQDs and with nonradiative energy transfer (FRET) from CQDs to metal NPs [25, 30].

The measurements showed that, in the presence of plasmonic NPs, the intensity of the CQDs DF decreases almost twice. Its duration was also reduced (Table 2).

Registration of the oxygen phosphorescence kinetics showed that in the presence of plasmonic NPs, its intensity in solutions of carbon particles increases by almost 2 times (Fig. 5). The greatest enhancement was recorded at a silver concentration of 10^{-13} mol/L. The lifetime did not change and amounted to 9.3±0.2 μs.

Table 2

Ag NPs effect on optical density, intensity and lifetime of fluorescence and DF of CQDs (75 % of ethanol) and phosphorescence of $O_2(^1\Delta_g)$ at atmospheric pressure

C_{Ag}, mol/L	D	I_{fl}, r.u.	τ_{fl}±0.1, ns	I_{DF}, r.u. 430 nm	τ_{DF}±0.2, μs 430 nm	I, r.u. 1270 nm	τ±0.2, μs 1270 nm
0	0.17	52.90	8.70	480.00	29.7	111.5	9.35
10^{-15}	0.17	50.86	8.14	380.50	24.5	163.3	9.34
10^{-14}	0.17	50.10	8.10	360.50	24.4	168.0	9.26
10^{-13}	0.17	49.90	7.85	324.00	24.2	202.0	9.35
10^{-12}	0.17	47.10	8.00	354.50	25.8	176.0	9.44

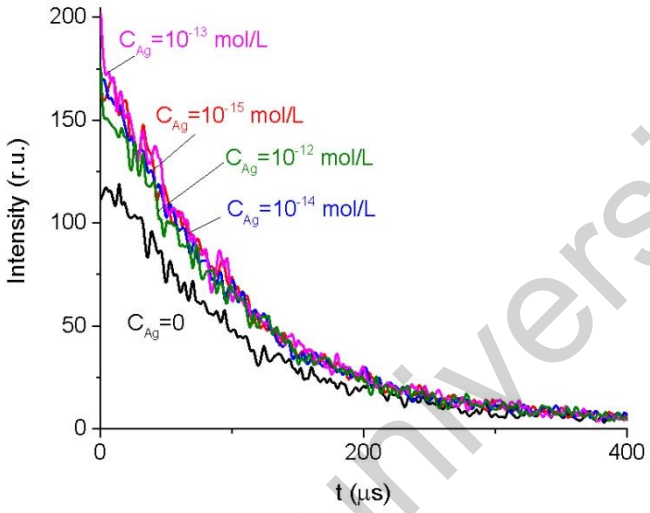

Figure 5. Decay kinetics of sensitized phosphorescence of $O_2(^1\Delta_g)$ (λ_{reg}=1270 nm) at different concentrations of Ag NPs in solution

Possible reasons for the enhancement of oxygen phosphorescence may be the following. The plasmonic effect can increase the population of the CQDs triplet state, which will lead to an increase in the concentration of singlet oxygen. The effect of Ag NPs on the exchange of energy between CQDs species and $O_2(^3\Sigma_g^-)$ triplet molecules is also possible [49]. In addition, the plasmon effect can directly enhance the rate of radiative decay of singlet oxygen. Our further work will be devoted to a detailed establishment of the mechanisms of the influence of the plasmon effect of metal NPs on the photo-physics of molecular oxygen and CQDs.

Conclusions

The properties of the long-lived luminescence of CQDs solutions were studied. It was established that the decay of the CQDs triplet states occurs as a result of a radiative phosphorescent transition and triplet–triplet annihilation. The synthesized CQDs species are the singlet oxygen sensitizers, as evidenced by the observed luminescence of molecular oxygen upon excitation of solutions in the CQDs absorption band. It was shown that the addition of aerated $O_2(^3\Sigma_g^-)$ to the solution leads to the development of the process of singlet–triplet annihilation, the efficiency of which depends on the concentrations ratio of triplet CQDs and the singlet $O_2(^1\Delta_g)$ molecules. In the presence of plasmonic Ag NPs, the phosphorescence of singlet oxygen is enhanced.

Acknowledgments

This research is funded by the Science Committee of the Ministry of Science and Higher Education of the Republic of Kazakhstan (Grant No. AP09259913).

References

1 Pibiri, I., Buscemi, S., Palumbo Piccionello, A. & Pace, A. (2017). Photochemically produced singlet oxygen: applications and perspectives. *ChemPhotoChem*, *2*(7), 535–547. https://doi.org/10.1002/cptc.201800076

2 Bregnhøj, M., Westberg, M., Minaev, B. F. & Ogilby, P. R. (2017). Singlet oxygen photophysics in liquid solvents: converging on a unified picture. *Acc. Chem. Res.*, *50*, 1920–1927. https://doi.org//10.1021/acs.accounts.7b00169.

3 Minaev, B. F. (2007). Electronic mechanisms of activation of molecular oxygen. *Russ. Chem. Rev.*, *76*(1), 989. https://doi.org/10.1070/RC2007v076n11ABEH003720

4 Minaev, B. F., Minaeva, V. A. & Evtuhov, Y. V. (2009). Quantum chemical study of the singlet oxygen emission. *Int. J. Quantum Chem.*, *109*, 500–515. https://doi.org/10.1002/qua.21783

5 Minaev, B. F., Murugan, N. A. & Ågren, H. (2013). Dioxygen spectra and bioactivation. *Int. J. Quantum Chem.*, *113*, 1847–1867. https://doi.org/10.1002/qua.24390

6 Minaev, B.F. (2022). The spin of dioxygen as the main factor in pulmonology and respiratory care. *Arch. Pulmonol. Respir. Care*, *8(1)*, 028–033. https://dx.doi.org/10.17352/aprc.000081

7 Maharjan, P. S. & Bhattarai, H. K. (2022). Singlet oxygen, photodynamic therapy, and mechanisms of cancer cell death. J. Oncology, 2022, 7211485. https://doi.org/10.1155/2022/7211485

8 Ishchenko, A. A. & Syniugina, A. T. (2023). Structure and photosensitaizer ability of polymethine dyes in photodynamic therapy: a Review. *Theor. Exp. Chem.*, *58*, 373–401. https://doi.org/10.1021/acs.bioconjchem.9b00482

9 Jiang, Y., Fu, Y., Xu, X., Guo, X., Wang, F., Xu, X., Yao-Wei, Huang, Shi, J. & Shen, C. (2023). Production of singlet oxygen from photosensitizer erythrosine for facile inactivation of coronavirus on mask. *Environment Int.*, *177*, 107994. https://doi.org/10.1016/j.envint.2023.107994

10 Schmidt, R. Photosensitized generation of singlet oxygen. (2006). *Photochem Photobiol.*, *82*(5), 1161–1177. https://dx.doi.org/10.1562/2006-03-03-IR-833.

11 Aerssens, D., Cadoni, E., Tack, L. & Madder, A. (2022). A Photosensitized singlet oxygen ($^1O_2$) toolbox for bio-organic applications: tailoring $^1O_2$ generation for DNA and protein labelling, targeting and biosensing. *Molecules, 27(3)*, 778. https://www.mdpi.com/1420-3049/27/3/778

12 Sheng, F., Ling, J., Hong, R., Jin, X., Wang, C., Zhong, H., Gu, X. & Gu, C. (2019). A new pathway of monomethylmercury photodegradation mediated by singlet oxygen on the interface of sediment soil and water. Environ. Pollut., *248*, 667–675. https://doi.org/10.1016/j.envpol.2019.02.047

13 Wan, B. & Lu, S. (2022). The light of carbon dots: From mechanism to application. *Matter*, *5*, 110–149. https://doi.org/10.1016/j.matt.2021.10.016.

14 Song, S. H., Jang, M. H., Chung, J., Jin, S. H., Kim, B. H., Hur, S. H., Yoo, S., Cho, Y. & Jeon, S. (2014). Highly efficient light-emitting diode of graphene quantum dots fabricated from graphite intercalation compounds. *Adv. Opt. Mater.*, *11*, 1016–1023. https://doi.org/10.1002/adom.201400184

15 Sun, Q. C., Dinga, Y. C., Sagara, D. M. & Nagpal, P. (2017). Photon upconversion towards applications in energy conversion and bioimaging. *Prog. Surf. Sci.*, *92*, 281–316. https://doi.org/10.1016/j.progsurf.2017.09.003

16 Kang, H., Zheng, J., Liu, X. & Yang, Y. (2021). Phosphorescent carbon dots: microstructure design, synthesis and applications. *New Carbon Mater.*, *36*, 649–664. https://doi.org/10.1016/s1872-5805(21)60083-5

17 Kim, A., Dash, J. K., Kumar, P. & Patel, R. (2022). Carbon-based quantum dots for photovoltaic devices: a review. *ACS Appl. Electron. Mater.*, *4*, 27–58. https://doi.org/10.1021/acsaelm.1c00783

18 Sciortino, A., Mauro, N., Buscarino, G., Sciortino, L., Popescu, R., Schneider, R., Giammona, G., Gerthsen, D., Cannas, M. & Messina, F. (2018). β-C_3N_4 nanocrystals: carbon dots with extraordinary morphological, structural, and optical homogeneity. *Chem. Mater.*, *30*, 1695–1700. https://doi.org/10.1021/acs.chemmater.7b05178

19 Nur Afifah, A. N., Nur Hidayah, A., Mohd Hafiz, A. B., Nadhratun, N. M., Yunhan, L., Norhana, A., Hasnan Tg, A. A., Ahmad Rifqi, Md Z. & Ahmad Ashrif, A. B. (2022). Localized surface plasmon resonance decorated with carbon quantum dots and triangular Ag nanoparticles for chlorophyll detection. *Nanomaterials*, *12*, 35. https://doi.org/10.3390/nano12010035

20 Sun, H., Gao, N., Dong, K., Ren, J. & Qu, X. (2014). Graphene quantum dots-band-aids used for wound disinfection. *ACS Nano*, *8*, 6202-6210. https://doi.org/10.1021/nn501640q

21 Fowley, C., Nomikou, N., McHale, A.P., McCaughan, B. & Callan, J.F. (2013). Extending the tissue penetration capability of conventional photosensitisers: a carbon quantum dotprotoporphyrin IX conjugate for use in two-photon excited photodynamic therapy. *Chem. Commun.*, *49*, 8934-8936. https://doi.org/10.1039/C3CC45181J

22 Zhou, Y., Sun, H., Wang, F., Ren, J. & Qu, X. (2017). How functional groups influence ROS generation and cytotoxicity of graphene quantum dots. *Chem. Comm.*, *53*, 10588-10591. https://doi.org/10.1039/C7CC04831A

23 Pillar-Little, T. J., Wanninayake, N., Nease, L., Heidary, D. K., Glazer, E. C. & Kim, D. Y. (2018). Superior photodynamic effect of carbon quantum dots through both type I and type II pathways: detailed comparison study of top-down-synthesized and bottom-up-synthesized carbon quantum dots. *Carbon*, *140*, 616-623. https://doi.org/10.1016/j.carbon.2018.09.004

24 Wu, S., Zhou, R., Chen, H., Zhang, J. & Wu, P. (2020). Highly efficient oxygen photosensitization of carbon dots: the role of nitrogen doping. *Nanoscale*, *12*, 5543–5553. https://doi.org/10.1039/C9NR10986B

25 Seliverstova, E., Ibrayev, N., Omarova, G., Ishchenko, A. & Kucherenko, M. (2021). Competitive influence of the plasmon effect and energy transfer between chromophores and Ag nanoparticles on the fluorescent properties of indopolycarbocyanine dyes. *J. Lumin.*, *235*, 118000. https://doi: 10.1016/j.jlumin.2021.118000

26 Ibrayev, N., Afanasyev, D., Ishchenko, A. & Kanapina, A. (2021). Influence of silver nanoparticles on the spectral-luminescent and lasing properties of merocyanine dyes solutions. *Laser Phys. Lett.*, *18*, 085001. https://doi.org/10.1088/1612-202X/ac0e3f

27 Yu, H., Peng, Y., Yang, Y. & Li, Z. (2019). Plasmon-enhanced light–matter interactions and applications. *NpjComput. Mater.*, *5*, 45. https://doi:10.1038/s41524-019-0184-1

28 Seliverstova, E. V., Ibrayev N. K. & Zhumabekov, A. Zh. (2020). The effect of silver nanoparticles on the photodetecting properties of the TiO_2/graphene oxide nanocomposite. *Opt. Spectrosc.*, *128*, 1449–1457. https://doi:10.1134/S0030400X20090192

29 Bitton, O., Gupta, S. & Haran, G. (2019). Quantum dot plasmonics: from weak to strong coupling. *Nanophotonics*, *8*, 559–575. https://doi:10.1515/nanoph-2018-0218

30 Temirbayeva, D., Ibrayev, N. & Kucherenko, M. (2022). Distance dependence of plasmon-enhanced fluorescence and delayed luminescence of molecular planar nanostructures. *J. Lumin.*, *243*, 118642. https://doi:10.1016/j.jlumin.2021.118642

31 Lakowicz, J. R. (2006). Principles of Fluorescence Spectroscopy, N.Y.: Kluwer Plenum Publishers.

32 Anger, P., Bharadwaj, P. & Novotny, L. (2006). Enhancement and quenching of single–molecule fluorescence. *Phys. Rev. Lett.*, *96*, 113002. https://doi.org/10.1103/PhysRevLett.96.113002

33 Yuan, K., Qin, R., Yu, J., Li, X., Li, L., Yang, X. & Liu H. (2019). Effects of localized surface plasmon resonance of Ag nanoparticles on luminescence of carbon dots with blue, green and yellow emission. *Appl. Surf. Sci.*, *502*, 144277. https://doi:10.1016/j.apsusc.2019.144277

34 Bagra, B., Zhang, W., Zeng, Z., Mabe, T. & Wei, J. (2019). Plasmon enhanced fluorescence of carbon nanodots in gold nanoslit cavities. *Langmuir*, *35*, 8903-8909. https://doi:10.1021/acs.langmuir.9b00448

35 Kamura, Y. & Imura, K. (2020). Photoluminescence from carbon dot-gold nanoparticle composites enhanced by photonic and plasmonic double-resonant effects. *ACS Omega*, *5*, 29068-29072. https://doi.org/10.1021/acsomega.0c03588

36 Sciortino, A., Panniello, A., Minervini, G., Mauro, N, Giammona, G., Buscarino, G., Cannas, M., Striccoli, M. & Messina, F. (2022). Enhancing carbon dots fluorescence via plasmonic resonance energy transfer. *Mater. Res. Bull. 149*, 111746. https://doi.org/10.1016/j.materresbull.2022.111746

37 Abdolmohammad-Zadeh, H., Azari, Z. & Pourbasheer, E. (2020). Fluorescence resonance energy transfer between carbon quantum dots and silver nanoparticles: Application to mercuric ion sensing. *Spectrochim. Acta A.*, *245*, 118924. https://doi.org/10.1016/j.saa.2020.118924

38 Nazri, N., Azeman, N., Bakar, M., Mobarak, N., Luo, Y., Arsad, N., Aziz, T., Zain, A. & Bakar, A. (2022). Localized surface plasmon resonance decorated with carbon quantum dots and triangular Ag nanoparticles for chlorophyll detection. *Nanomaterials*, *12*, 35. https://doi.org/10.3390/nano12010035

39 Bukasov, R., Filchakova, O., Gudun, K. & Bouhrara, M. (2017). Strong surface enhanced florescence of carbon dot labeled bacteria cells observed with high contrast on gold film. *J. Fluoresc*, *28*, 1–4. https://doi.org/10.1007/s10895-017-2194-z

40 Amjadi, M., Shokri, R. & Hallaj, T. (2016). Interaction of glucose-derived carbon quantum dots with silver and gold nanoparticles and its application for the fluorescence detection of 6-thioguanine. *Luminescence*, *32*, 292–297. https://doi.org/10.1002/bio.3177

41 Ibrayev, N., Dzhanabekova, R., Seliverstova, E. & Amanzholova, G. (2021). Optical properties of N- and S-doped carbon dots based on citric acid and L-cysteine. *Fullerenes, Nanotubes, Carbon Nanostruct.*, *30(1)*, 22-26. https://doi.org/10.1080/1536383X.2021.1999933

42 Liu, J., Zhang, H., Wang, N., Yu, Y., Cui, Y., Li, J. & Yu, J. (2019). Template-modulated afterglow of carbon dots in zeolites: room-temperature phosphorescence and thermally activated delayed fluorescence. *ACS Materials Lett.*, *1*, 58–63. https://doi.org/10.1021/acsmaterialslett.9b00073

43 Zhang, H., Wang, B., Yu, X., Li, J., Shang, J. & Yu, J. (2020). Carbon dots in porous materials: host–guest synergy for enhanced performance. *Angew. Chemie Inernat. Ed.*, *59(44)*, 19390-19402. https://doi.org/10.1002/anie.202006545

44 Buchachenko, A. L., Sagdeev, R. Z. & Salikhov K. M. (1978). Magnitniye spinovye effecty v khimicheskikh reaktsiiakh [Magnetic spin effects in chemical reactions]. Novosibirsk: Nauka [in Russian].

45 Bregnhøj, M., Westberg, M., Jensen, F. & Ogilby, P. R. (2016). Solvent-dependent singlet oxygen lifetimes: temperature effects implicate tunneling and charge-transfer interactions. *Phys. Chem. Chem. Phys.*, *18*, 22946-22961. https://doi.org/10.1039/C6CP01635A

46 Salokhiddinov, K. I., Byteva, I. M. & Gurinovich, G. P. (1981). Lifetime of singlet oxygen in various solvents. *J. Appl. Spectrosc.*, *34*, 561–564. https://doi.org/10.1007/BF00613067

47 Minaev, B. F. (1985). Quantum-chemical investigation of the mechanisms of the photosensitization, luminescence, and quenching of singlet $^1\Delta_g$ oxygen in solutions. *J. Appl. Spectrosc*., *42*(5), 518-523. https://doi.org/10.1007/BF00661398

48 Minaev, B. F., Lunell, S. & Kobzev, G. I. (1994). Collision-induced intensity of the $b^1\Sigma_g^+ - a^1\Delta_g$ transition in molecular oxygen: Model calculations for the collision complex O_2+ H_2. *Int. J. Quantum Chem.*, *50*(4), 279-292. https://doi.org/10.1002/qua.560500405

49 Bryukhanov, V. V., Minaev, B. F., Tsibul'nikova, A. V. & Slezhkin V. A. (2015). The Effect of gold nanoparticles on exchange processes in collision complexes of triplet and singlet oxygen molecules with excited eosin molecules. *Optics Spectrosc., 119(1),* 29–38. https://doi.org/10.1134/S0030400X15070061

50 Konstantinova, E. I., Minaev, B. F., Tsibul'nikova, A. V., Borkunov, Yu. R., Tsar'kov, M. V., Antipov, Yu., Samusev, I. G. & Bryukhanov, V. V. (2018). Dynamics of thermoluminescence under dual-wavelength vis–ir laser excitation of eosin molecules in a polyvinyl butyral film containing oxygen and silver nanoparticles. *Optics Spectrosc., 125(6),* 874–881. https://doi.org/10.1134/S0030400X19020152

Information about authors*

Ibrayev, Niyazbek Khamzauly (*corresponding author*) — Doctor of Physical-Mathematical Sciences, Institute of Molecular Nanophotonics, Karaganda University of the name of academician E.A. Buketov, Universitetskaya street, 28, 100024, Karaganda, Kazakhstan; e-mail: niazibrayev@mail.ru; https://orcid.org/0000-0002-5156-5015

Seliverstova, Evgeniya Vladimirovna — Doctor PhD, Institute of Molecular Nanophotonics, Karaganda University of the name of academician E.A. Buketov, Universitetskaya street, 28, 100024, Karaganda, Kazakhstan; e-mail: genia_sv@mail.ru; https://orcid.org/0000-0002-9507-8825

*The author's name is presented in the order: *Last Name, First and Middle Names*